

Generalization of generative model for neuronal ensemble inference method

Shun Kimura* Koujin Takeda*[†]

7th November, 2022

Abstract

Various brain functions that are necessary to maintain life activities materialize through the interaction of countless neurons. Therefore, it is important to analyze the structure of functional neuronal network. To elucidate the mechanism of brain function, many studies are being actively conducted on the structure of functional neuronal ensemble and hub, including all areas of neuroscience. In addition, recent study suggests that the existence of functional neuronal ensembles and hubs contributes to the efficiency of information processing. For these reasons, there is a demand for methods to infer functional neuronal ensembles from neuronal activity data, and methods based on Bayesian inference have been proposed. However, there is a problem in modeling the activity in Bayesian inference. The features of each neuron's activity have non-stationarity depending on physiological experimental conditions. As a result, the assumption of stationarity in Bayesian inference model impedes inference, which leads to destabilization of inference results and degradation of inference accuracy. In this study, we extend the expressivity of the model in the previous study and improve it to a soft clustering method, which can be applied to activity data with non-stationarity. In addition, for the effectiveness of the method, we apply the developed method to synthetic data generated by the leaky-integrate-and-fire model, and discuss the result.

Keywords: neuronal network, neuronal ensemble, Bayesian inference, Markov chain Monte Carlo method, Dirichlet process

*Department of Mechanics Systems Engineering, Graduate School of Science and Engineering, Ibaraki University, Hitachi, Ibaraki, Japan

[†]koujin.takeda.kt@vc.ibaraki.ac.jp

Introduction

In many organisms, various functions necessary to maintain life activities such as perception, movement, and emotion are realized through the interaction of countless neurons in multiple regions of brain. Each neuron transmits information by chemical and electrical signals through synaptic and gap junctions. Therefore, from the perspective of network science, structure analysis of neuronal network is important for elucidating the mechanisms of brain functions. As such, in many fields of neuroscience, various studies are being conducted to elucidate the structure of neuronal networks from experimental and theoretical viewpoints. In fact, in the field of neurophysiology, measurement techniques have been developed for the purpose of simultaneously visualizing the activity of neurons in multiple brain regions. One of the main methods for macroscopically measuring neuronal activity at the level of a single neuron is calcium imaging, which can measure the activity of a large number of neurons on the 10^4 order at a time[14].

The strength of functional connection, namely the target for inferring network structure, changes from moment to moment and is non-stationary due to the features of neuronal activity. This means that responses to stimuli are different due to various brain states such as sleep and wakefulness, which are internal states of organisms. However, in the currently proposed methods for network structure inference, the functional connection strength is often evaluated as time-averaged quantity[11, 16, 17]. In addition, since there can be connections between unobserved and observed neurons in experiments, it is possible that the activity of unobserved neurons influences the activity of observed ones. Therefore, it is very difficult to estimate the strength of functional connectivity from unprocessed activity data.

Given this, various methods for inferring functional neuronal ensembles, which are groups of neurons with synchronous activity, have been proposed for clarifying global structure of network. It can also be used for limiting the data to be analyzed as preprocessing of local network structure inference[9, 10, 2, 15, 12]. Among these methods, Bayesian inference model and Markov chain Monte Carlo (MCMC) method are used in the previous study[3], whose improvement for faster convergence to inference result is also proposed [8]. As another topic, it has been suggested that hub neurons, which have connections with many neurons and influence them in neuronal network, are involved in the efficiency of the information processing mechanism between neurons [5]. Thus, the inferences of the functional neuronal ensemble centered on hub neurons and network structure inside and outside the ensemble are important not only as a preprocessing for inference of local network structure but also for elucidating the global mechanism of brain

functions.

As mentioned above, inference of functional neuronal ensemble is a common goal in the field of neuroscience. However, the method based on Bayesian inference needs a generative model, where only binary expression of neuronal activity data is allowed in the previous study. Accordingly, it cannot be applied to activity data of continuous values such as fluorescence intensity by calcium imaging. It is possible to apply to continuous value data after binarization preprocessing. However it is desirable to directly analyze continuous value data, because part of the original information in activity data may be lost by binarization. In addition, Bayesian inference model in the previous study assumes stationarity in the activity of each neuron, which means that the structure of functional neuronal ensemble is assumed to be unchanged under the measurement experiment. Therefore, when such inference method is applied to highly non-stationary activity data with frequent changes of brain states such as sleep and wakefulness, the inference result may not be stable due to the dependence on initial condition in MCMC and the inference accuracy may worsen. Additionally, destabilization of the result and degradation of accuracy are also due to hard clustering method in the previous study.

For these reasons, we develop a generalized method in this study, which does not depend on the format of the input neuronal activity data and can be implemented as a soft clustering method. Specifically, we extend the expressivity of generative model for neuronal activity in Bayesian inference and develop an algorithm using MCMC for the extended model. For validity, we apply the proposed method to synthetic neuronal activity data generated by the leaky-integrate-and-fire model[6], which is known as a model of neuronal activity. Then we finally discuss the results of application.

Materials and methods

Bayesian inference model

The notation of variables in this article is based on the previous work [3]. Boldface is used to denote a vector or matrix variable unless otherwise specified. Additionally, subscript is used to denote each element in a vector or matrix variable.

In our model, let N be the number of neurons, M be the number of time steps in activity measurement, and A be the number of neuronal ensembles. The generative model in the proposed Bayesian inference method is expressed using three variables: \mathbf{s} is neuronal activity; \mathbf{t} is the weight of a neuron

belonging to a neuronal ensemble; and $\boldsymbol{\omega}$ is time-series activity state of a neuronal ensemble. The subscripts i , k , and μ used in elementwise notation of each variable represent the label of the neuron, the label of the time step, and the label of the neuronal ensemble, respectively. Therefore, each variable represents the following.

- s_{ik} : neuronal activity of the i -th neuron at the k -th time step
- $t_{\mu i}$: membership weight of the i -th neuron to the μ -th ensemble
- $\omega_{k\mu}$: activity of the μ -th ensemble at the k -th time step

The ranges of variables \boldsymbol{s} and $\boldsymbol{\omega}$ are limited as $0 \leq s_{ik} \leq 1 \forall i, k$ and $0 \leq \omega_{k\mu} \leq 1 \forall k, \mu$, respectively, to normalize the activity weights of each neuron and ensemble. The variable $\boldsymbol{t}_i = \{t_{1i}, \dots, t_{Ai}\}$ is one-hot representation or $t_{\mu i} \in \{0, 1\}$ in the case of hard clustering, while $t_{\mu i}$ ranges from 0 to 1 and satisfies $\sum_{\mu=1}^A t_{\mu i} = 1 \forall i$ in the case of soft clustering.

In addition to these variables, three parameters \boldsymbol{n} , \boldsymbol{p} , and $\boldsymbol{\lambda}$ are introduced to each ensemble in the generative model, whose meanings are described in the following. For each parameter, Dirichlet or beta distribution is assumed as prior distribution to facilitate marginalization in Bayesian inference.

- \boldsymbol{n} : affinity parameter to a neuronal ensemble, following Dirichlet distribution
- \boldsymbol{p} : activity parameter of a neuronal ensemble, following beta distribution
- $\boldsymbol{\lambda}$: synchrony parameter between the activities of a neuronal ensemble and neurons within the ensemble, following beta distribution

More precisely, two kinds of $\boldsymbol{\lambda}$'s are introduced for synchrony; $\boldsymbol{\lambda}_1$ or $\boldsymbol{\lambda}_0$ is the synchrony when both of ensemble and neuron are active or inactive, respectively. The distribution of parameters in this model is expressed as follows.

$$P(n_1, \dots, n_A | \alpha_1^{(n)}, \dots, \alpha_A^{(n)}) = \text{Dir} \left(\alpha_1^{(n)}, \dots, \alpha_A^{(n)} \right) \propto \prod_{\mu=1}^A n_{\mu}^{\alpha_{\mu}^{(n)} - 1}, \quad (1)$$

$$P(p_{\mu} | \alpha_{\mu}^{(p)}, \beta_{\mu}^{(p)}) = \text{Beta} \left(\alpha_{\mu}^{(p)}, \beta_{\mu}^{(p)} \right) \propto p_{\mu}^{\alpha_{\mu}^{(p)} - 1} (1 - p_{\mu})^{\beta_{\mu}^{(p)} - 1}, \quad (2)$$

$$P(\lambda_{1,\mu} | \alpha_{1,\mu}^{(\lambda)}, \beta_{1,\mu}^{(\lambda)}) = \text{Beta} \left(\alpha_{1,\mu}^{(\lambda)}, \beta_{1,\mu}^{(\lambda)} \right) \propto \lambda_{1,\mu}^{\alpha_{1,\mu}^{(\lambda)} - 1} (1 - \lambda_{1,\mu})^{\beta_{1,\mu}^{(\lambda)} - 1} \quad (3)$$

$$P(\lambda_{0,\mu} | \alpha_{0,\mu}^{(\lambda)}, \beta_{0,\mu}^{(\lambda)}) = \text{Beta} \left(\alpha_{0,\mu}^{(\lambda)}, \beta_{0,\mu}^{(\lambda)} \right) \propto \lambda_{0,\mu}^{\alpha_{0,\mu}^{(\lambda)} - 1} (1 - \lambda_{0,\mu})^{\beta_{0,\mu}^{(\lambda)} - 1} \quad (4)$$

where $\alpha_\mu^{(n)}, \alpha_\mu^{(p)}, \beta_\mu^{(p)}, \alpha_{1,\mu}^{(\lambda)}, \beta_{1,\mu}^{(\lambda)}, \alpha_{0,\mu}^{(\lambda)}, \beta_{0,\mu}^{(\lambda)}$ are hyperparameters.

The likelihood is designed as follows to facilitate marginalization like the design of prior distribution.

$$\begin{aligned}
& P(\mathbf{t}, \boldsymbol{\omega}, \mathbf{s} | \mathbf{n}, \mathbf{p}, \boldsymbol{\lambda}) \\
& \propto \left(\prod_{\mu=1}^A n_{\mu}^{\tilde{\alpha}_\mu^{(n)}} \right) \cdot \left(\prod_{\mu=1}^A p_{\mu}^{\tilde{\alpha}_\mu^{(p)}} (1 - p_{\mu})^{\tilde{\beta}_\mu^{(p)}} \right) \\
& \cdot \left(\prod_{\mu=1}^A \left[\lambda_{1,\mu}^{\tilde{\alpha}_{1,\mu}^{(\lambda)}} (1 - \lambda_{1,\mu})^{\tilde{\beta}_{1,\mu}^{(\lambda)}} \right] \right) \cdot \left(\prod_{\mu=1}^A \left[\lambda_{0,\mu}^{\tilde{\alpha}_{0,\mu}^{(\lambda)}} (1 - \lambda_{0,\mu})^{\tilde{\beta}_{0,\mu}^{(\lambda)}} \right] \right), \quad (5)
\end{aligned}$$

where

$$\tilde{\alpha}_\mu^{(n)} = \sum_{i=1}^N t_{\mu i}, \quad (6)$$

$$\tilde{\alpha}_\mu^{(p)} = \sum_{k=1}^M \omega_{k\mu}, \quad (7)$$

$$\tilde{\beta}_\mu^{(p)} = \sum_{k=1}^M (1 - \omega_{k\mu}), \quad (8)$$

$$\tilde{\alpha}_{1,\mu}^{(\lambda)} = \sum_{k=1}^M \omega_{k\mu} \sum_{i=1}^N t_{\mu i} s_{ik}, \quad (9)$$

$$\tilde{\beta}_{1,\mu}^{(\lambda)} = \sum_{k=1}^M \omega_{k\mu} \sum_{i=1}^N t_{\mu i} (1 - s_{ik}), \quad (10)$$

$$\tilde{\alpha}_{0,\mu}^{(\lambda)} = \sum_{k=1}^M (1 - \omega_{k\mu}) \sum_{i=1}^N t_{\mu i} s_{ik}, \quad (11)$$

$$\tilde{\beta}_{0,\mu}^{(\lambda)} = \sum_{k=1}^M (1 - \omega_{k\mu}) \sum_{i=1}^N t_{\mu i} (1 - s_{ik}). \quad (12)$$

Note that they are defined by the variables $\mathbf{t}, \boldsymbol{\omega}$, and \mathbf{s} . For inference, we need the joint distribution of $\mathbf{t}, \boldsymbol{\omega}$, and \mathbf{s} under given hyperparameters. By product rule in Bayesian statistics and marginalization of the parameters

$\mathbf{n}, \mathbf{p}, \boldsymbol{\lambda}$, the following expression is obtained,

$$\begin{aligned}
& P(\mathbf{t}, \boldsymbol{\omega}, \mathbf{s} | \boldsymbol{\alpha}^{(n)}, \boldsymbol{\alpha}^{(p)}, \boldsymbol{\beta}^{(p)}, \boldsymbol{\alpha}_1^{(\lambda)}, \boldsymbol{\beta}_1^{(\lambda)}, \boldsymbol{\alpha}_0^{(\lambda)}, \boldsymbol{\beta}_0^{(\lambda)}) \\
&= \int d\mathbf{n} d\mathbf{p} d\boldsymbol{\lambda} P(\mathbf{t}, \boldsymbol{\omega}, \mathbf{s}, \mathbf{n}, \mathbf{p}, \boldsymbol{\lambda} | \boldsymbol{\alpha}^{(n)}, \boldsymbol{\alpha}^{(p)}, \boldsymbol{\beta}^{(p)}, \boldsymbol{\alpha}_1^{(\lambda)}, \boldsymbol{\beta}_1^{(\lambda)}, \boldsymbol{\alpha}_0^{(\lambda)}, \boldsymbol{\beta}_0^{(\lambda)}) \\
&= \int d\mathbf{n} d\mathbf{p} d\boldsymbol{\lambda} P(\mathbf{t}, \boldsymbol{\omega}, \mathbf{s} | \mathbf{n}, \mathbf{p}, \boldsymbol{\lambda}) \\
&\quad \cdot P(\mathbf{n}, \mathbf{p}, \boldsymbol{\lambda} | \boldsymbol{\alpha}^{(n)}, \boldsymbol{\alpha}^{(p)}, \boldsymbol{\beta}^{(p)}, \boldsymbol{\alpha}_1^{(\lambda)}, \boldsymbol{\beta}_1^{(\lambda)}, \boldsymbol{\alpha}_0^{(\lambda)}, \boldsymbol{\beta}_0^{(\lambda)}) \\
&\propto \int d\mathbf{n} d\mathbf{p} d\boldsymbol{\lambda} \left(\prod_{\mu=1}^A n_{\mu}^{\{\alpha_{\mu}^{(n)} + \tilde{\alpha}_{\mu}^{(n)}\} - 1} \right) \\
&\quad \cdot \prod_{\mu=1}^A \left(p_{\mu}^{\{\alpha_{\mu}^{(p)} + \tilde{\alpha}_{\mu}^{(p)}\} - 1} (1 - p_{\mu})^{\{\beta_{\mu}^{(p)} + \tilde{\beta}_{\mu}^{(p)}\} - 1} \right) \\
&\quad \cdot \left(\lambda_{1,\mu}^{\{\alpha_{1,\mu}^{(\lambda)} + \tilde{\alpha}_{1,\mu}^{(\lambda)}\} - 1} (1 - \lambda_{1,\mu})^{\{\beta_{1,\mu}^{(\lambda)} + \tilde{\beta}_{1,\mu}^{(\lambda)}\} - 1} \right) \\
&\quad \cdot \left(\lambda_{0,\mu}^{\{\alpha_{0,\mu}^{(\lambda)} + \tilde{\alpha}_{0,\mu}^{(\lambda)}\} - 1} (1 - \lambda_{0,\mu})^{\{\beta_{0,\mu}^{(\lambda)} + \tilde{\beta}_{0,\mu}^{(\lambda)}\} - 1} \right) \\
&= \mathcal{B} \left(\alpha_1^{(n)} + \tilde{\alpha}_1^{(n)}, \dots, \alpha_A^{(n)} + \tilde{\alpha}_A^{(n)} \right) \prod_{\mu=1}^A B \left(\alpha_{\mu}^{(p)} + \tilde{\alpha}_{\mu}^{(p)}, \beta_{\mu}^{(p)} + \tilde{\beta}_{\mu}^{(p)} \right) \\
&\quad B \left(\alpha_{1,\mu}^{(\lambda)} + \tilde{\alpha}_{1,\mu}^{(\lambda)}, \beta_{1,\mu}^{(\lambda)} + \tilde{\beta}_{1,\mu}^{(\lambda)} \right) B \left(\alpha_{0,\mu}^{(\lambda)} + \tilde{\alpha}_{0,\mu}^{(\lambda)}, \beta_{0,\mu}^{(\lambda)} + \tilde{\beta}_{0,\mu}^{(\lambda)} \right), \quad (13)
\end{aligned}$$

where $B(x_1, x_2)$ is beta function and $\mathcal{B}(x_1, \dots, x_A)$ is multivariate beta function represented as

$$B(x_1, x_2) = \frac{\Gamma(x_1) \Gamma(x_2)}{\Gamma(x_1 + x_2)}, \quad (14)$$

$$\mathcal{B}(x_1, \dots, x_A) = \frac{\prod_{\mu=1}^A \Gamma(x_{\mu})}{\Gamma\left(\sum_{\mu=1}^A x_{\mu}\right)}, \quad (15)$$

with $\Gamma(x)$ being gamma function. For inference of the structure of the functional neuronal ensemble and activity of the ensemble, namely inference of \mathbf{t} and $\boldsymbol{\omega}$, the marginalized expression (13) is used for improvement of inference accuracy and reduction of computational cost.

MCMC and Dirichlet process

In our method, the structure of the neuronal ensemble and activity of ensemble are inferred from the solution of posterior maximization by applying

MCMC method to Eq (13) similarly to the previous study [3]. In addition, the number of neuronal ensembles is dynamically changed by Dirichlet process in MCMC. Dirichlet process is a stochastic process that can generate arbitrary discrete distributions, and the probability of each event is determined by concentration parameter [13]. For speeding up the inference by MCMC, parallel computation using synchronous update is implemented.

The variables to be inferred are \mathbf{t} and $\boldsymbol{\omega}$ in our model, and the variable updates for \mathbf{t} and $\boldsymbol{\omega}$ are performed alternately until convergence in MCMC. The flow of variable update is summarized as follows.

1. The ensemble activity $\boldsymbol{\omega}$ is updated according to Metropolis-Hastings method in MCMC.
2. The value of the membership weight \mathbf{t} is updated according to Dirichlet process and Metropolis-Hastings method in MCMC.
3. The hyperparameters are updated using updated $\boldsymbol{\omega}$ and \mathbf{t} by the processes 1 and 2.

The update rule of membership weight $\mathbf{t}_i = \{t_{1i}, \dots, t_{Ai}\}$ is explained in the following, which differs from the previous study due to the change of the generative model. Other variables are updated in the same manner as in the previous study.

In our model, the element of membership weight $t_{\mu i}$ is a continuous variable satisfying normalization condition $\sum_{\mu=1}^A t_{\mu i} = 1$. Hence, for update of membership weight \mathbf{t}_i , all elements in \mathbf{t}_i must be updated unlike Dirichlet process for one-hot representation of \mathbf{t}_i in the previous study. Let \mathbf{t}_i^0 be the original membership weight of neuron i before update and \mathbf{t}_i^* be the proposed membership weight for update, which may or may not be accepted by Metropolis-Hastings method. Here we define *concentration ensemble* G_i^* for neuron i in each iteration of MCMC. The values in elements of the proposed membership weights \mathbf{t}_i^* will concentrate on the ensemble G_i^* by Dirichlet process with *transition parameter* α . More precisely, in Dirichlet process the concentration ensemble G_i^* is determined first, next the weight $t_{G_i^* i}$ is increased by α and the weights of other ensembles remain unchanged, then finally all elements of the proposed weight are normalized so as to satisfy the condition of probability. In the case of hard clustering as in the previous study, such normalization is not necessary because of one-hot representation of the weight.

The concentration ensemble G_i^* is determined according to the transition probability in Dirichlet process as in the following Eq (16). The probability for the concentration ensemble G_i^* is proportional to the size of the ensemble

G_i^* , that is, the sum of the proposed weights of the neurons belonging to the ensemble G_i^* [13, 7].

$$Q(G_i^*|\mathbf{t}^0) = \frac{\sum_{j=1, j \neq i}^N t_{G_i^* j}^*}{N-1}, \quad (16)$$

where $\mathbf{t}^0 = \{\mathbf{t}_1^0, \dots, \mathbf{t}_N^0\}$. Then, the proposed weights are computed as in Eq (17), which includes the increase of the weight $t_{G_i^*}$ and the normalization.

$$t_{\mu i}^* = \begin{cases} \frac{t_{\mu i}^0}{1+\alpha} & \text{if } \mu \neq G_i^*, \\ \frac{t_{\mu i}^0 + \alpha}{1+\alpha} & \text{if } \mu = G_i^*. \end{cases} \quad (17)$$

Conversely, to satisfy the detailed balance condition in MCMC, the reverse process for the determination of concentration ensemble must be considered. The probability of concentration ensemble before update, denoted by G_i^0 , is expressed by Eq (18) under given membership weight after update, namely \mathbf{t}_i^* .

$$Q(G_i^0|\mathbf{t}_i^*, \mathbf{t}_{\setminus i}^0) = \frac{\sum_{j=1, j \neq i}^N t_{G_i^0 j}^0}{N-1}, \quad (18)$$

where backslash means removal of specific element, $\mathbf{t}_{\setminus i}^0 = \{\mathbf{t}_1^0, \dots, \mathbf{t}_{i-1}^0, \mathbf{t}_{i+1}^0, \dots, \mathbf{t}_N^0\}$. Therefore, the ratio of probabilities for the concentration ensembles G_i^*, G_i^0 is given by

$$\frac{Q(G_i^0|\mathbf{t}_i^*, \mathbf{t}_{\setminus i}^0)}{Q(G_i^*|\mathbf{t}^0)} = \frac{\sum_{j=1, j \neq i}^N t_{G_i^0 j}^0}{\sum_{j=1, j \neq i}^N t_{G_i^* j}^*}. \quad (19)$$

The derived probabilities ratio is represented by the ratio of the ensemble sizes. Remember that \mathbf{t}_i^* is the proposed membership weight, and for acceptance of the proposed weight it is necessary to calculate the acceptance rate in Metropolis-Hastings method. The acceptance rate of the proposed weight \mathbf{t}_i^* under the original weight \mathbf{t}_i^0 is given as

$$a(\mathbf{t}_i^*, \mathbf{t}_i^0) = \min \left(1, \frac{P(\mathbf{t}_i^*, \mathbf{t}_{\setminus i}^0, \boldsymbol{\omega}, \mathbf{s})}{P(\mathbf{t}_i^0, \boldsymbol{\omega}, \mathbf{s})} \frac{Q(G_i^0|\mathbf{t}_i^*, \mathbf{t}_{\setminus i}^0)}{Q(G_i^*|\mathbf{t}^0)} \right), \quad (20)$$

where hyperparameters in P are omitted and

$$\begin{aligned}
& \frac{P(\mathbf{t}_i^*, \mathbf{t}_{\setminus i}^0, \boldsymbol{\omega}, \mathbf{s}) Q(G_i^0 | \mathbf{t}_i^*, \mathbf{t}_{\setminus i}^0)}{P(\mathbf{t}^0, \boldsymbol{\omega}, \mathbf{s}) Q(G_i^* | \mathbf{t}^0)} \\
= & \frac{\mathcal{B}\left(\alpha_1^{(n)} + \tilde{\alpha}_1^{(n)}, \dots, \alpha_A^{(n)} + \tilde{\alpha}_A^{(n)}\right) \Big|_{\mathbf{t}_i = \mathbf{t}_i^*}}{\mathcal{B}\left(\alpha_1^{(n)} + \tilde{\alpha}_1^{(n)}, \dots, \alpha_A^{(n)} + \tilde{\alpha}_A^{(n)}\right) \Big|_{\mathbf{t}_i = \mathbf{t}_i^0}} \\
& \frac{\prod_{\mu=1}^A B\left(\alpha_{1,\mu}^{(\lambda)} + \tilde{\alpha}_{1,\mu}^{(\lambda)}, \beta_{1,\mu}^{(\lambda)} + \tilde{\beta}_{1,\mu}^{(\lambda)}\right) B\left(\alpha_{0,\mu}^{(\lambda)} + \tilde{\alpha}_{0,\mu}^{(\lambda)}, \beta_{0,\mu}^{(\lambda)} + \tilde{\beta}_{0,\mu}^{(\lambda)}\right) \Big|_{\mathbf{t}_i = \mathbf{t}_i^*}}{\prod_{\mu=1}^A B\left(\alpha_{1,\mu}^{(\lambda)} + \tilde{\alpha}_{1,\mu}^{(\lambda)}, \beta_{1,\mu}^{(\lambda)} + \tilde{\beta}_{1,\mu}^{(\lambda)}\right) B\left(\alpha_{0,\mu}^{(\lambda)} + \tilde{\alpha}_{0,\mu}^{(\lambda)}, \beta_{0,\mu}^{(\lambda)} + \tilde{\beta}_{0,\mu}^{(\lambda)}\right) \Big|_{\mathbf{t}_i = \mathbf{t}_i^0}} \\
& \frac{\sum_{j=1, j \neq i}^N t_{G_i^0 j}}{\sum_{j=1, j \neq i}^N t_{G_i^* j}}. \tag{21}
\end{aligned}$$

Once the variables are updated, the hyperparameters are also updated using updated $\boldsymbol{\omega}$ and \mathbf{t} . The hyperparameters to be updated are $\alpha_\mu^{(n)}$, which is related to membership of neuron, $\alpha_\mu^{(p)}, \beta_\mu^{(p)}$, which are related to ensemble activity, and $\alpha_{1,\mu}^{(\lambda)}, \beta_{1,\mu}^{(\lambda)}, \alpha_{0,\mu}^{(\lambda)}, \beta_{0,\mu}^{(\lambda)}$, which are related to synchrony between activities of ensemble and neurons. For instance, the update rule of $\alpha_\mu^{(n)}$ is given as follows,

$$\hat{\alpha}_\mu^{(n)} = \alpha_\mu^{(n)} + \tilde{\alpha}_\mu^{(n)}, \tag{22}$$

where $\hat{\alpha}_\mu^{(n)}$ is updated hyperparameter. Other hyperparameters are also updated similarly.

Results

We conduct numerical experiment for the effectiveness and the validity of the proposed method by applying to continuous value data. For experiment, synthetic neuronal activity data is generated by the leaky-integrate-and-fire model, which is known as a model of neuronal activity. We should compare the result of experiment with the previous study, however application of the inference method in the previous study is limited to binary data. Therefore, when applying the two methods to synthetic continuous value data, raw continuous data is used in the proposed method and the binarized one is used in the method of the previous study.

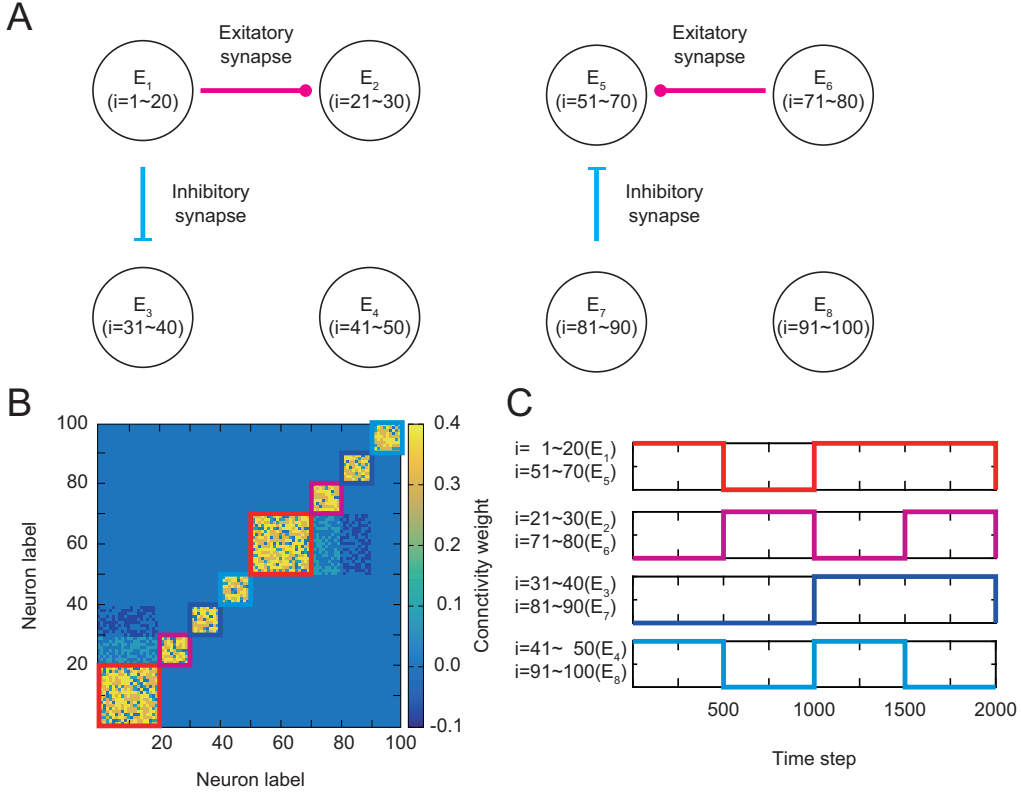


Figure 1: Ensemble structure of neurons. A: Connections between ensembles. B: Heat map of weights between neurons. C: Patterns of input currents.

Generation of synthetic data

The leaky-integrate-and-fire model is known as describing the states of neurons with electrical and chemical interactions [6]. In this model, the electric current inputs from other neurons are integrated as the electric potential until it exceeds the threshold. When it exceeds, a sudden rise of potential called spike firing occurs. This phenomenon is expressed by the form of a differential equation.

In the experiment, we generate synthetic data with $N = 100$, $M = 2000$, $A = 8$, and with ensemble structure of E_1 to E_8 shown in Fig 1A. The ensemble sizes are not uniform in the data; two ensembles E_1 and E_5 have 20 neurons and others have 10 neurons. The neurons in the same ensemble are connected randomly by excitatory synaptic connections, while the neurons in different ensembles are connected by design; excitatory connections $E_1 \rightarrow E_2$, $E_6 \rightarrow E_5$ and inhibitory connections $E_1 \rightarrow E_3$, $E_7 \rightarrow E_5$. Therefore,

Table 1: Conditions of experiment

	previous study	proposed method
number of initial ensembles: A_{init}	50	16
number of trials: r_{max}	16	16
number of updates in MCMC: γ_{max}	1000	1000
concentration parameter: α	none	$\{0.1, 0.3, 0.5\}$

the connections between neurons differ depending on the ensemble as shown in Fig 1B. In addition, an input current with a different pattern is given as in Fig 1C to each ensemble.

Fig 2A is a heat map representation of the continuous-valued synthetic data generated under the above-mentioned setting of connections. In contrast, Fig 2B shows the data after binarization, which is obtained by inferring spike signals from local maximum value of the activity and by performing binarization. Here we use Findpeaks function in MATLAB library to find local maximum of the activity. This binarized data is used for comparison with the method in the previous study. As expected, the activities of neurons in the same ensemble tend to be similar in Fig 2A. In Fig 2B, the activities in the same ensemble are also similar like in Fig 2A, therefore we believe there is no problem in data preprocessing by binarization. Furthermore, it can be observed that the activities of neurons in downstream ensembles of connections, namely E_2, E_3, E_5 in our setting, tend to be disturbed by the neurons in upstream ensembles, E_1, E_6, E_7 . Additionally, as in Fig 2A and 2B, synthetic activity data of all neurons is non-stationary, which reflects non-stationarity of the input current.

Results of the application

We apply the two methods to synthetic data; our proposed method and the one in the previous study[3]. For performance evaluation of ensemble inference, the average of multiple trials with different initial conditions is taken, because the dependence of MCMC result on initial condition should be removed as much as possible. In the method of the previous study, the number of initial ensembles is set to half the number of neurons as recommended, which is to avoid convergence to an inappropriate local solution. Other conditions are the same between the two methods. The detailed conditions of the experiment are summarized in Table 1.

For the behavior by multiple trials, we observe how often each neuron is classified into the same ensemble, for which we define the similarity matrix

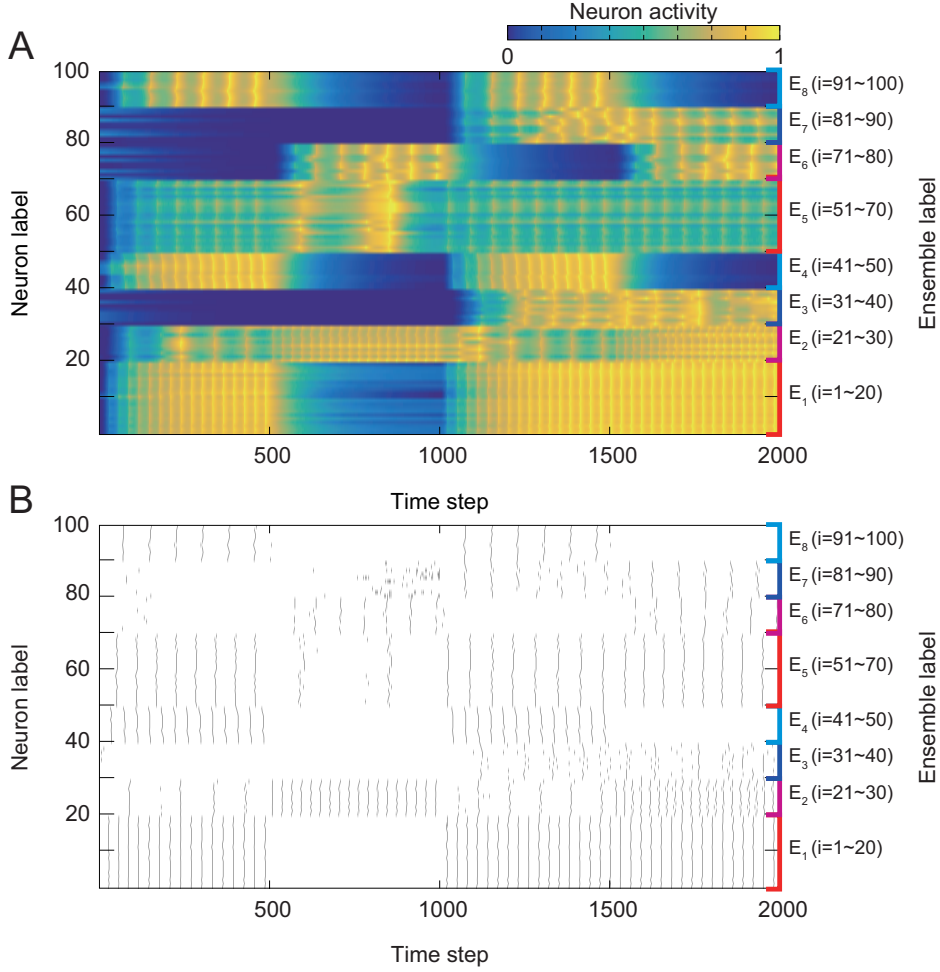


Figure 2: Synthetic activity data to be analyzed. A: Continuous activity data by the neurons with the connections in Fig 1. B: Activity data after binarization. Black/white point indicates active/inactive neuron, respectively.

F. The element of \mathbf{F} represents the similarity of activities between neurons, which reflects ensemble structure averaged over multiple trials. Element of the similarity matrix is expressed as $F_{ij} = \sum_{r=1}^{r_{\max}} \sum_{\mu=1}^{A_{\text{init}}} t_{\mu i}^r t_{\mu j}^r$, where r is the label of trial with initial condition being changed.

Fig 3A, 3B, and 3C are the heat map of the matrix element F_{ij} with the values of the transition parameter being varied. The element F_{ij} is obtained by applying the proposed method to the data in Fig 2A. In contrast, Fig 3D is the result by applying the method in the previous study to the binary data in Fig 2B.

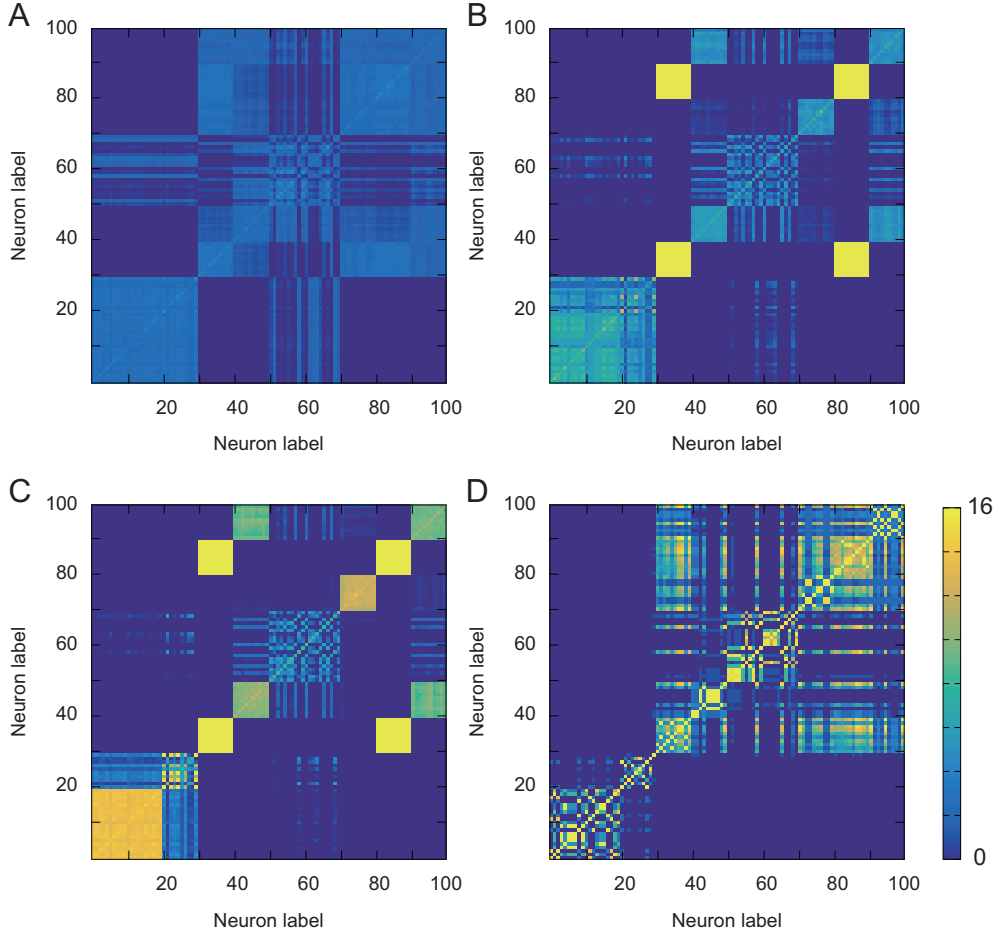


Figure 3: Heat map of \mathbf{F} by the proposed method and the method in previous study. A: $\alpha = 0.1$ (proposed) B: $\alpha = 0.3$ (proposed) C: $\alpha = 0.5$ (proposed) D: The result by the method in the previous study

Discussion

As can be observed in Fig 3A, 3B, and 3C, the ensemble structure is changed by the value of the transition parameter α . For example, when focusing on neurons $i = 1 \sim 30$ in E_1 and E_2 , the coarse-grained large ensemble structure is obtained under small α as in Fig 3A, where the original two ensembles E_1 and E_2 are merged. In contrast, detailed ensemble structure is obtained under large α as in Fig 3C, where E_1 and E_2 are separated. Furthermore, in the proposed method we observe the groups of neurons in different original ensembles, for example the neurons in the ensemble pair E_3, E_7 or another

pair E_4, E_8 , are classified into the merged ensemble, although there is no structural connection between these original ensembles. The neurons in such ensemble pair have similar neuronal activity as in Fig 2, because the same electric current is provided as the input into the ensemble pair and the activity is not easily affected by the input due to the structure of connection between ensembles. In the proposed method, the inference of ensemble structure is based only on synchrony of neuronal activity. Thus, even if there is no structural connection, these neurons with similar activity are classified into the same ensemble as a consequence.

On the other hand, when the method in previous study is applied to the activity data after binarization, only the course-grained ensemble structure can be found in Fig 3D. It is difficult to discriminate ensembles with similar activity by this method, because this method can only be used as hard clustering and does not have extra parameter to control hard/soft clustering like transition parameter in the proposed method.

Conclusion

In this study, we extended the inference model for functional neuronal ensemble to be applicable regardless of data format and stationarity. The purpose of the proposed method is to classify neurons into the ensembles by using large-scale activity data acquired by experimental method such as calcium imaging. For that reason, no restriction on the format of the activity or no assumption of stationarity due to physiological experimental conditions is desirable. Therefore, the proposed method without restriction on format or stationarity assumption will function effectively and can be widely used as a method of data preprocessing. By the application of the proposed method to the same synthetic data multiple times, we confirmed that it converges to a reasonable and sufficiently stable solution, although the proposed method has dependence on initial condition due to MCMC. In addition, by the comparison of the proposed method with the one in the previous study, we believe that our proposed method is more useful to obtain the ensemble structure and the relationship between ensembles by adjusting the transition parameter α .

The inference method for functional neuronal ensembles in our study or in the previous study can be considered as preprocessing for clarifying functional *network* structure between neurons, whose experimental size is recently increasing [3]. Therefore, network structure inference with the aid of information of functional neuronal ensemble is a future topic of our study. As existing methods of network inference, the method using spin-glass model, which is to describe the ordered states of magnetic materials with impurities

in the field of statistical physics [11, 16, 17], and the method of graph analysis for graphical representation of similarity between neurons [1, 18, 4] are known for example. However, stationarity of network structure is assumed in many network inference methods. In addition, input neuronal activity is often limited to binary in these methods, and they cannot be applied to continuous value data such as fluorescence intensity by calcium imaging. Therefore, they are not sufficient as models to express functional connections between neurons with non-stationarity. For the use of our proposed method as preprocessing of network inference, the first issue to be considered is to generalize the network inference method without restriction of data format or stationarity assumption of input activity.

Acknowledgments

This work is supported by KAKENHI Nos. 18K11175, 19K12178, 20H05774, and 20H05776.

References

- [1] Lilach Avitan, Zac Pujic, Jan Mölter, Matthew Van De Poll, Biao Sun, Haotian Teng, Rumelo Amor, Ethan K Scott, and Geoffrey J Goodhill. Spontaneous activity in the zebrafish tectum reorganizes over development and is influenced by visual experience. *Current Biology*, 27(16):2407–2419, 2017.
- [2] Luis Carrillo-Reid, Jae-eun Kang Miller, Jordan P Hamm, Jesse Jackson, and Rafael Yuste. Endogenous sequential cortical activity evoked by visual stimuli. *Journal of Neuroscience*, 35(23):8813–8828, 2015.
- [3] Giovanni Diana, Thomas TJ Sainsbury, and Martin P Meyer. Bayesian inference of neuronal assemblies. *PLOS Computational Biology*, 15(10):e1007481, 2019.
- [4] Owen Forbes, Edgar Santos-Fernandez, Paul Pao-Yen Wu, Hong-Bo Xie, Paul E. Schwenn, Jim Lagopoulos, Lia Mills, Dashiell D. Sacks, Daniel F. Hermens, and Kerrie Mengersen. clusterbma: Bayesian model averaging for clustering. *arXiv preprint arXiv:2209.04117v1*, 2022.
- [5] Eyal Gal, Oren Amsalem, Alon Schindel, Michael London, Felix Schürmann, Henry Markram, and Idan Segev. The role of hub neu-

- rons in modulating cortical dynamics. *Frontiers in Neural Circuits*, 15, 2021.
- [6] Wulfram Gerstner, Werner M Kistler, Richard Naud, and Liam Paninski. *Neuronal dynamics: From single neurons to networks and models of cognition*. Cambridge University Press, 2014.
- [7] Sonia Jain and Radford M Neal. A split-merge markov chain monte carlo procedure for the dirichlet process mixture model. *Journal of Computational and Graphical Statistics*, 13(1):158–182, 2004.
- [8] Shun Kimura, Keisuke Ota, and Koujin Takeda. Improved neuronal ensemble inference with generative model and mcmc. *Journal of Statistical Mechanics: Theory and Experiment*, 2021(6):063501, 2021.
- [9] Vítor Lopes-dos Santos, Sergio Conde-Ocazonez, Miguel AL Nicolelis, Sidarta T Ribeiro, and Adriano BL Tort. Neuronal assembly detection and cell membership specification by principal component analysis. *PLOS ONE*, 6(6):e20996, 2011.
- [10] Vítor Lopes-dos Santos, Sidarta Ribeiro, and Adriano BL Tort. Detecting cell assemblies in large neuronal populations. *Journal of Neuroscience Methods*, 220(2):149–166, 2013.
- [11] Marc Mézard and J Sakellariou. Exact mean-field inference in asymmetric kinetic ising systems. *Journal of Statistical Mechanics: Theory and Experiment*, 2011(07):L07001, 2011.
- [12] Jan Mölter, Lilach Avitan, and Geoffrey J Goodhill. Detecting neural assemblies in calcium imaging data. *BMC Biology*, 16(1):1–20, 2018.
- [13] Radford M Neal. Markov chain sampling methods for dirichlet process mixture models. *Journal of Computational and Graphical Statistics*, 9(2):249–265, 2000.
- [14] Keisuke Ota, Yasuhiro Oisi, Takayuki Suzuki, Muneki Ikeda, Yoshiki Ito, Tsubasa Ito, Hiroyuki Uwamori, Kenta Kobayashi, Midori Kobayashi, Maya Odagawa, et al. Fast, cell-resolution, contiguous-wide two-photon imaging to reveal functional network architectures across multi-modal cortical areas. *Neuron*, 109(11):1810–1824, 2021.
- [15] Sebastián A Romano, Thomas Pietri, Verónica Pérez-Schuster, Adrien Jouary, Mathieu Haudrechy, and Germán Sumbre. Spontaneous neuronal network dynamics reveal circuit’s functional adaptations for behavior. *Neuron*, 85(5):1070–1085, 2015.

- [16] Yasser Roudi and John Hertz. Mean field theory for nonequilibrium network reconstruction. *Physical Review Letters*, 106(4):048702, 2011.
- [17] Yu Terada, Tomoyuki Obuchi, Takuya Isomura, and Yoshiyuki Kabashima. Inferring neuronal couplings from spiking data using a systematic procedure with a statistical criterion. *Neural Computation*, 32(11):2187–2211, 2020.
- [18] Hang Yin, Xinyue Liu, and Xiangnan Kong. Gaussian mixture graphical lasso with application to edge detection in brain networks. In *2020 IEEE International Conference on Big Data (Big Data)*, pages 1430–1435. IEEE, 2020.